Catalysis Today 183 (2012) 52–57

Contents lists available at SciVerse ScienceDirect

Catalysis Today

journal homepage: www.elsevier.com/locate/cattod

Preparation of vanadium phosphate catalyst precursors for the selective oxidation of butane using α,ω-alkanediols

Xiao-Bing Fan[a,b], Nicholas F. Dummer[a], Stuart H. Taylor[a], Jonathan K. Bartley[a,*], Graham J. Hutchings[a,*]

[a] School of Chemistry, Cardiff University, Cardiff CF10 3AT, UK
[b] College of Chemistry and Molecular Engineering, Peking University, Beijing 100871, China

ARTICLE INFO

Article history:
Received 1 July 2011
Received in revised form 13 August 2011
Accepted 15 August 2011
Available online 19 September 2011

Keywords:
Vanadium pyrophosphate
α,ω-Alkanediols
Butane
Selective oxidation
Intercalation

ABSTRACT

Vanadium phosphate catalyst precursors were prepared from V_2O_5 and H_3PO_4 or $VOPO_4{\cdot}2H_2O$ using α,ω-alkanediols (1,4-butanediol, 1,5-pentanediol and 1,6-hexanediol) as both the reducing agent and the solvent. A series of layered $VOHPO_4{\cdot}HO(CH_2)_nOH$ (n = 4–6) materials intercalated with α,ω-alkanediols were obtained. The performance for butane oxidation of the final catalysts formed *via* the *in situ* transformation of the $VOHPO_4{\cdot}HO(CH_2)_nOH$ precursors under reaction conditions is described. The final catalysts derived from the alkanediol intercalated materials were found to exhibit relatively low selectivities to maleic anhydride and comprised of V^V ($VOPO_4$) phases with an amorphous V^{IV} phase. However, when a crystalline $(V^{IV}O)_2P_2O_7$ phase is present, with small amounts of V^V phases, as with materials prepared with 1,4-butanediol, the specific and intrinsic catalytic activity are higher.

1. Introduction

Vanadium phosphates are important industrial catalysts that are used for the selective oxidation of butane to maleic anhydride [1,2]. Vanadium pyrophosphate, $(VO)_2P_2O_7$, is thought to be the active phase for butane oxidation and this is typically prepared by calcination of the precursor, $VOHPO_4{\cdot}0.5H_2O$ [3–5], although there is evidence which indicates that the surface of these catalysts is amorphous [6–9]. The morphology of the precursor is maintained in the final catalyst as the transformation is topotactic. Therefore, the preparation of $VOHPO_4{\cdot}0.5H_2O$ materials with high surface areas and different morphologies are of interest. The main strategy for the synthesis of $VOHPO_4{\cdot}0.5H_2O$ involves the reduction of $VOPO_4{\cdot}2H_2O$ or a mixture of V_2O_5 and H_3PO_4 with an alcohol. The nature of the alcohol can have a large influence on the morphology [10] and the mechanism for the precursor formation has been studied [11,12].

Vanadium phosphates intercalated with alcohols [13] and amides [14] have been studied as novel layered materials. The intercalation of α,ω-alkanediols into $VOPO_4{\cdot}2H_2O$ has been studied previously by Beneš et al. [15]. Since each α,ω-alkanediol molecular has two hydroxyl groups at the terminal position of the alkane chain, they show very different properties from alcohols when intercalated into $VOPO_4{\cdot}2H_2O$. Previously, attempts to modify the morphology of $VOHPO_4{\cdot}0.5H_2O$ with various α,ω-alkanediols used isobutanol as a co-solvent [16,17]. Taufiq-Yap and co-workers [18,19] reported the use of ethylene glycol as a reducing agent, resulting in an improved surface area. Following this reduction step, refluxing with distilled water decreased the crystallite size of the $VOHPO_4{\cdot}0.5H_2O$ precursor. The selective oxidation of butane was reported to improve when compared to standard materials, which was proposed to be related to the mobility and availability of lattice oxygen species. The preparation of intercalated vanadium hydrogen phosphates with longer chain α,ω-alkanediols in the absence of a co-solvent has not, to our knowledge, been reported. In this paper we report the preparation of $VOHPO_4{\cdot}HO(CH_2)_nOH$ materials *via* the reduction of $VOPO_4{\cdot}2H_2O$, or directly from V_2O_5 and H_3PO_4, using α,ω-alkanediols with varying chain length and investigate these as catalysts for selective butane oxidation.

2. Experimental

2.1. Preparation of $VOPO_4{\cdot}2H_2O$

Vanadium phosphate dihydrate ($VOPO_4{\cdot}2H_2O$) was prepared according to the literature [20]. V_2O_5 (2.5 g) was refluxed with H_3PO_4 (85%, 15.0 ml, Aldrich) in water (60 ml) for 16 h. The yellow

* Corresponding authors.
E-mail addresses: bartleyjk@cf.ac.uk (J.K. Bartley), hutch@cardiff.ac.uk (G.J. Hutchings).

0920-5861/$ – see front matter © 2011 Elsevier B.V. All rights reserved.
doi:10.1016/j.cattod.2011.08.030

Table 1
Preparation conditions of the catalyst precursors.

Precursor	Method[a]	Solvent/reductant
VPDI	VPD	Isobutanol
VPD4	VPD	1,4-Butanediol
VPD5	VPD	1,5-Pentanediol
VPD6	VPD	1,6-Hexanediol
VPO4	VPO	1,4-Butanediol
VPO5	VPO	1,5-Pentanediol
VPO6	VPO	1,6-Hexanediol

[a] VPO = $V_2O_5 + H_3PO_4$ refluxed with solvent/reducing agent, VPD = $VOPO_4{\cdot}2H_2O$ refluxed with solvent/reducing agent.

solid was recovered by filtration, washed with acetone and then dried in air (110 °C, 16 h).

2.2. Preparation of $VOHPO_4{\cdot}HO(CH_2)_nOH$

$VOHPO_4{\cdot}HO(CH_2)_nOH$ was synthesized by two routes, described as the VPO and VPD methods [21]. The VPO method denotes the reduction of V_2O_5 in the presence of H_3PO_4 in organic media. In a typical experiment, V_2O_5 (2.5 g) and H_3PO_4 (3.49 g, aqueous 85 vol%, P:V = 1:1) were reacted for 16 h at 125 °C with stirring. The resultant blue solid was recovered by vacuum filtration, washed with acetone and dried (110 °C, 16 h). The VPD method involves the reduction of vanadium phosphate dihydrate, $VOPO_4{\cdot}2H_2O$, with an alcohol. In a typical experiment, $VOPO_4{\cdot}2H_2O$ (1.0 g) was reacted with α,ω-alkanediol (50:1 alcohol:V molar ratio) for 16 h at 125 °C. The resultant blue solid was recovered by vacuum filtration, washed with acetone and dried in air (110 °C, 8 h). The designations and preparation conditions for the different vanadium phosphate precursors are listed in Table 1.

2.3. Catalyst characterization

Powder X-ray diffraction (XRD) patterns were recorded using a Panalytical X'pert Pro diffractometer using Ni filtered CuK_α radiation (operating at 40 kV, 40 mA). Scans were in the range 10–80° 2θ. All patterns were indexed using the ICDD database (International Centre for Diffraction Data, Pennsylvania, USA). Raman spectra were obtained using a Renishaw inVia Raman Microscope fitted with a green Ar^+ laser (λ = 514.532 nm). Scanning electron microscopy (SEM) was performed using a Hitachi 326YO-N instrument. BET surface area measurements by nitrogen adsorption were carried out at −196 °C using a Micromeritics ASAP 2000 instrument.

2.4. Catalytic evaluation for butane oxidation

A micro-reactor was used to carry out catalyst testing for the oxidation of butane. A feedstock composition of 1.7% butane in air was fed at a rate of 10 ml min^{-1} into a stainless-steel tube reactor typically containing 0.20 g of precursor held in place by plugs of quartz wool. The reactor was heated to the reaction temperature at a ramp rate of 3 °C min^{-1}. Product analysis was by on-line GC (Varian 3800). Carbon balances obtained were typically 95–105%. Precursors were activated *in situ* at 400 °C for >72 h.

3. Results and discussion

3.1. Catalyst precursor characterization

A standard vanadium phosphate precursor, $VOHPO_4{\cdot}0.5H_2O$ (VPDI), was synthesized *via* the VPD method with isobutanol. The *d* spacing of the (0 0 1) reflection (hereafter denoted $d_{(001)}$) was determined to be 0.57 nm from the XRD pattern (Fig. 1a) and SEM analysis (Fig. 1b) confirmed that the material had a rosette structure with a particle size of 1–5 μm. The position of the (0 0 1) reflection is an indication of the interlayer spacing between the vanadium phosphate layers and so can be used to determine whether intercalation of the alcohols has occurred.

The low angle XRD patterns of the precursors produced *via* the VPD method with α,ω-alkanediols are shown in Fig. 2. The $d_{(001)}$ spacing was found to increase to 1.09 and 1.21 nm when the solvent used was 1,4-butanediol or 1,5-propanediol respectively. The multiple reflections observed at the (0 0 1) position in the pattern of VPD6 (Fig. 2) suggest that intercalated 1,6-hexandiol could adopt different conformations with different interlayer spacings. This has been observed previously for $VOPO_4{\cdot}2H_2O$ intercalated with benzyl alcohol [22]. These results indicate that a series of α,ω-alkanediol intercalated compounds with the general formula, $VOHPO_4{\cdot}HO(CH_2)_nOH$, had been formed. This demonstrates that α,ω-alkanediols have more affinity to the vanadium phosphate layers than mono-functionalised alcohols which typically form $VOHPO_4{\cdot}0.5H_2O$ even though the alcohol is in excess (V:alcohol molar ratio = 1:50) [21]. The stoichiometry of the intercalated material formed is based on thermal analysis performed by Beneš et al. [15] which was found to be 1:1 with respect to $VOHPO_4$. $VOHPO_4{\cdot}HO(CH_2)_nOH$ compounds were also synthesized *via* the VPO method using the α,ω-alkanediols. The increasing shift of the (0 0 1) reflection with increasing carbon number of the alkanediol is similar to the trend found for the materials prepared *via* the VPD route (Fig. 3). The relationship between the carbon chain length of

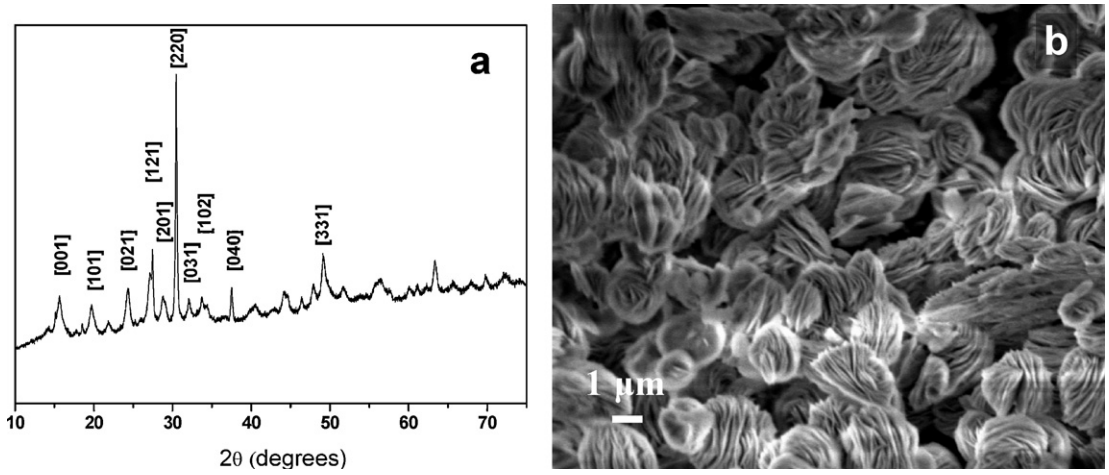

Fig. 1. (a) XRD pattern and (b) SEM image of the standard $VOHPO_4{\cdot}0.5H_2O$ precursor VPDI.

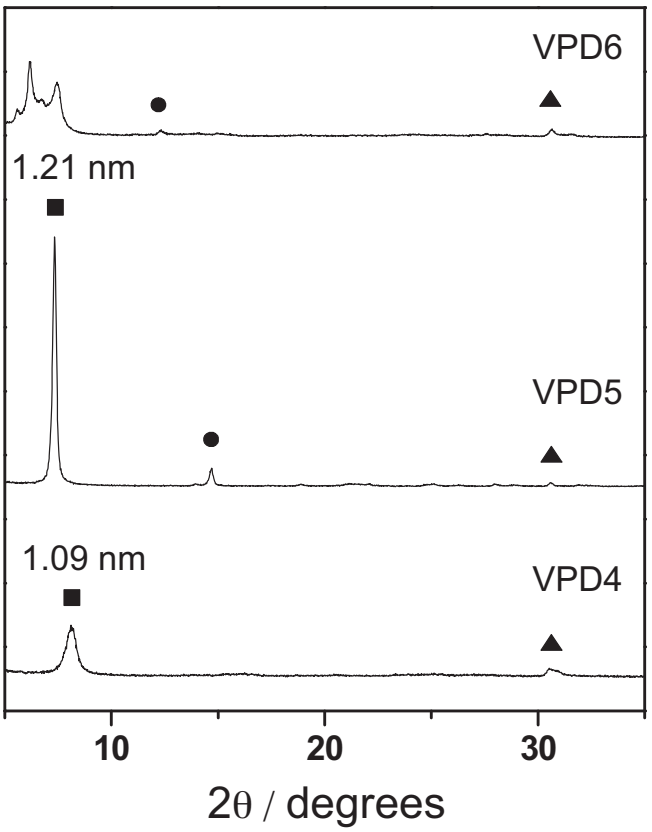

Fig. 2. Low angle XRD patterns of $VOHPO_4{\cdot}HO(CH_2)_nOH$ prepared by the VPD method with various α,ω-alkanediols. (0 0 1) = ■, with $d_{(001)}$ labelled; ● = (1 0 1) and ▲ = (2 2 0).

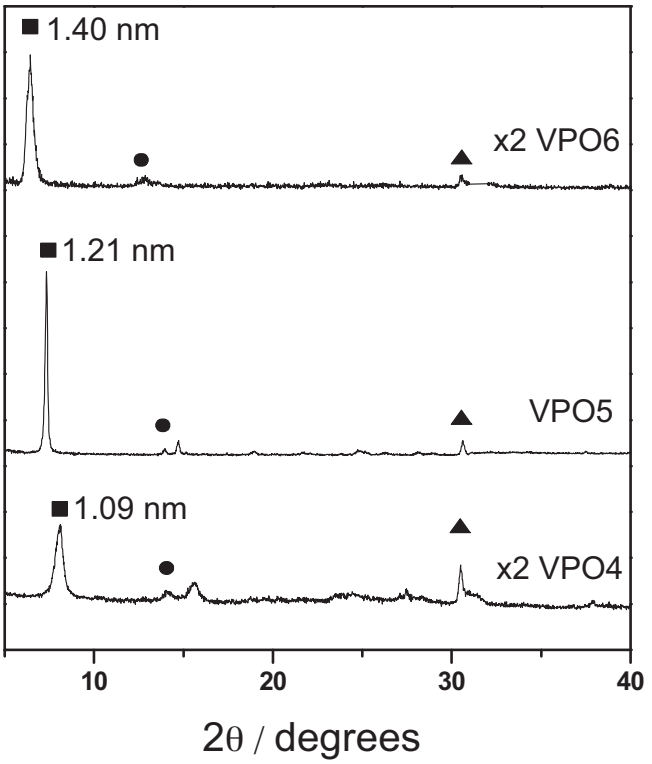

Fig. 3. Low angle XRD patterns of $VOHPO_4{\cdot}HO(CH_2)_nOH$ prepared by the VPO method with various α,ω-alkanediols. (0 0 1) = ■, with $d_{(001)}$ labelled: ● = (1 0 1) and ▲ = (2 2 0).

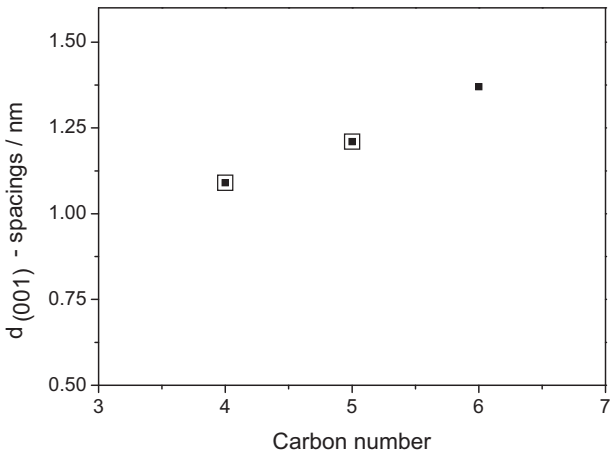

Fig. 4. The dependence of d_{001} of prepared materials (□ = VPD and ■ = VPO methodology) on the number of carbon atoms in the aliphatic chain of the α,ω-alkanediols used.

the alkanediol and $d_{(001)}$ are illustrated in Fig. 4. Changing the solvent from 1,4-butanediol to 1,6-hexandiol increased the observed $d_{(001)}$ from 1.09 to 1.4 nm. The $d_{(001)}$ value obtained for the materials prepared in this study are consistent with previous results. Beneš et al. [15] studied the intercalation of different alcohols into $VOPO_4{\cdot}2H_2O$ and concluded that bi-molecular layers were formed using mono-functionalised alcohols, while α,ω-alkanediols formed

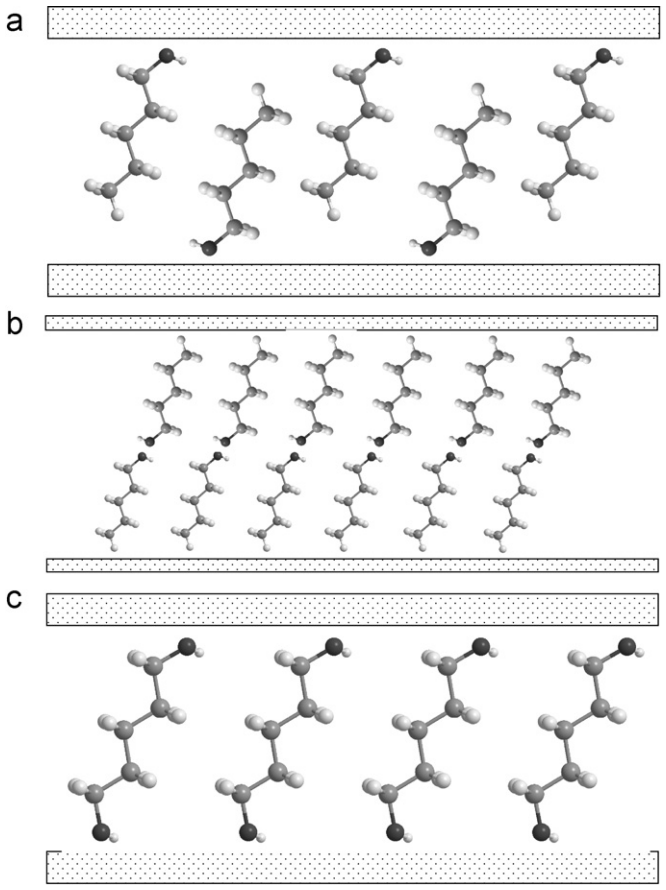

Fig. 5. Schematic representation of vanadium phosphate intercalation by a monomolecular layer of: (a) an alcohol, (b) bi-molecular layer of an alcohol and (c) a monomolecular layer of an α,ω-alkanediol. Adapted from [15], black spheres = oxygen, grey = carbon and white = hydrogen.

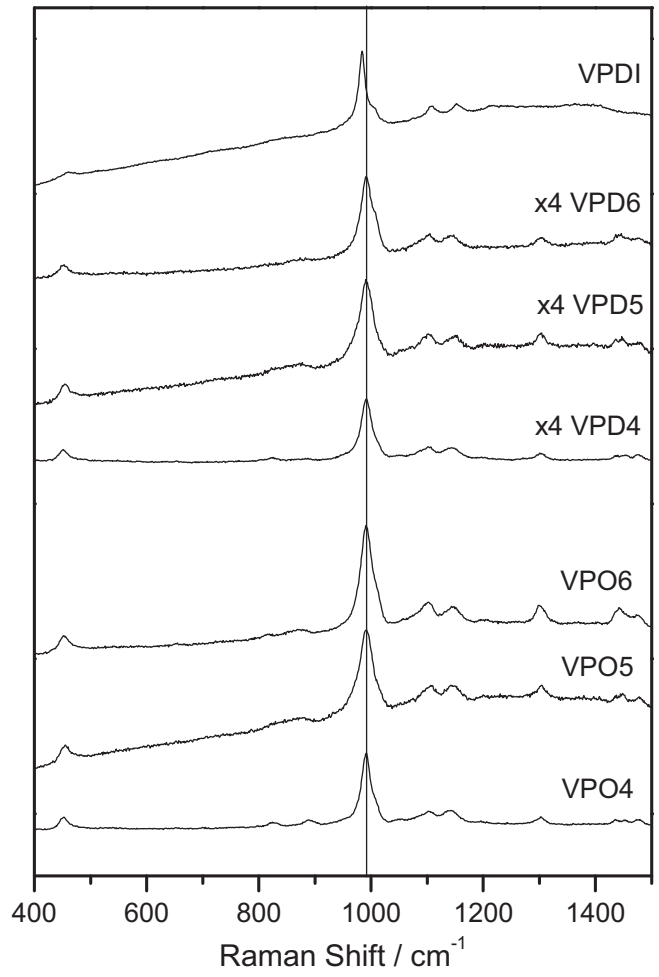

Fig. 6. Raman spectra of $VOHPO_4{\cdot}HO(CH_2)_nOH$ prepared with various α,ω-alkanediols and the standard catalyst precursor, $VOHPO_4{\cdot}0.5H_2O$ (VPDI). The line indicates υ(V=O) at 992 cm^{-1}.

mono-molecular layers between the vanadium phosphate sheets (Fig. 5).

Raman spectroscopy of the precursor samples indicated that the strong transition associated with υ(V=O) stretching at 984 cm^{-1} for VPDI has shifted in the case of the intercalated precursors to 992 cm^{-1} (Fig. 6). This shift in transition is indicative of a change in the V=O bond strength when an alcohol is coordinated to the vanadium atom compared with coordinated H_2O in the standard hydrated precursor.

The SEM images of the precursors (Figs. 7 and 8) show that they consist of aggregates comprised of thin sheets arranged to form rosette like structures. The origin and mechanism of the formation of this rosette morphology was studied by Mahoney et al. [11] and a mechanism was suggested that involved the insertion of isobutanol into $VOPO_4{\cdot}2H_2O$ to form curled sheets *via* delamination of the layers with $VOHPO_4{\cdot}0.5H_2O$ nucleation at the sheet edges. There are several alcohols that have been shown to reduce $VOPO_4{\cdot}2H_2O$ to give a rosette morphology, and in this study we observe a high degree of delamination of the $VOHPO_4{\cdot}HO(CH_2)_nOH$ samples. Interestingly, rosette-like particles were also produced *via* the VPO method. Typically, $VOHPO_4{\cdot}0.5H_2O$ synthesized *via* the reaction of V_2O_5, phosphoric acid and an alcohol forms particles with a platelet morphology [5]. In this study, vanadium (IV) phosphate rosette-like materials were formed, possibly due to increased delamination of the $VOHPO_4{\cdot}HO(CH_2)_nOH$ platelets by the intercalated α,ω-alkanediols.

3.2. Selective oxidation of butane

The synthesized materials were tested as catalysts for the partial oxidation of butane to maleic anhydride in a fixed-bed reactor following *in situ* activation of the precursors (Table 2). The XRD patterns of the catalysts post reaction are shown in Fig. 9. Most of the activated catalysts derived from the intercalated materials exhibited poor crystallinity and showed low intensity XRD reflections. In view of this, the detection of the many potential vanadium phosphate phases that could be present in the final catalysts was attempted with Raman spectroscopy. Comparing the Raman spectra (Fig. 10) and XRD patterns of various vanadium phosphate phases to those reported previously [23,24], it was found that the standard precursor $VOHPO_4{\cdot}0.5H_2O$ (VPDI) formed crystalline $(VO)_2P_2O_7$ during the reaction and gave a relatively high selectivity to maleic anhydride (*ca.* 58%). After reaction, there are low angle reflections in the XRD patterns of the catalysts derived from $VOHPO_4{\cdot}HO(CH_2)_nOH$. Although it cannot be unequivocally assigned to a particular phase, reflections at these low angles are associated with large *d*-spacings and are only observed in lamellar vanadium phosphate compounds with molecules such as H_2O between the layers. The Raman spectra (Fig. 10) show that not all of the precursor is reduced during activation leading to V^VOPO_4 phases in the final catalyst. After reaction, the $VOPO_4$ phases can adsorb atmospheric water and rehydrate to form layered $VOPO_4{\cdot}nH_2O$ structures, leading to the low angle reflections observed in the XRD patterns (Fig. 9). The catalysts derived from intercalated $VOHPO_4{\cdot}HOC_4H_8OH$ (VPD4 and VPO4) achieved selectivity to maleic anhydride of 36–47% and were found to contain crystalline $(VO)_2P_2O_7$ and V^V phases. These materials also have relatively high activities and surface areas compared with the precursors prepared with longer chain alkanediols. The post-reaction

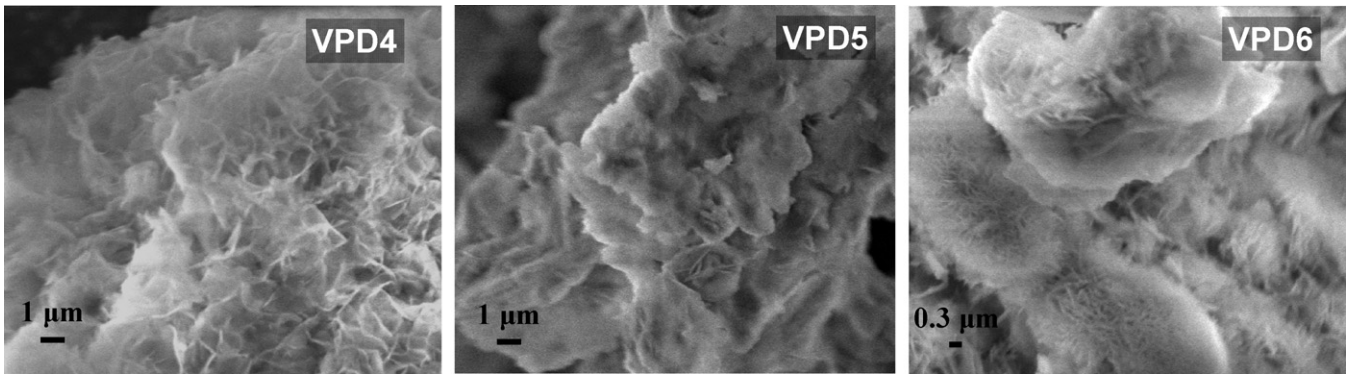

Fig. 7. SEM images of vanadium phosphate catalyst precursors prepared with various α,ω-alkanediols according to the VPD methodology.

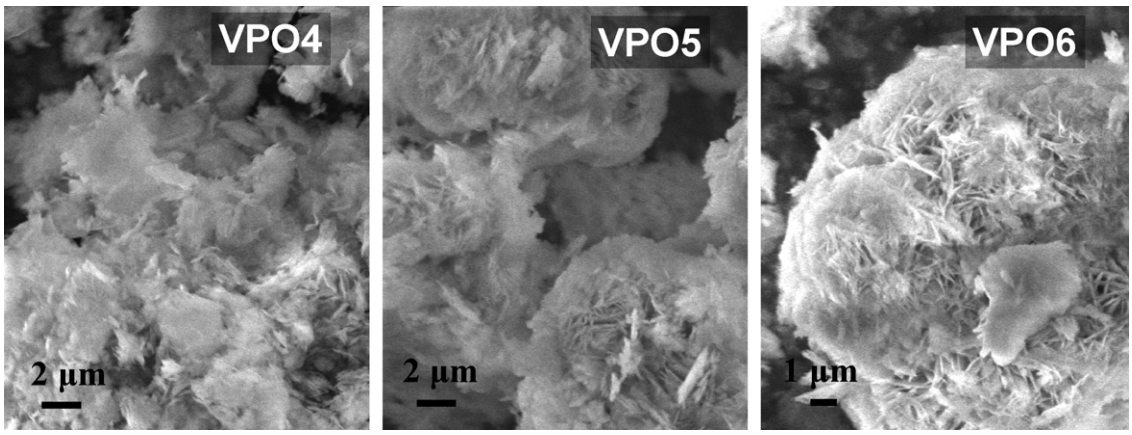

Fig. 8. SEM images of vanadium phosphate catalyst precursors prepared with various α,ω-alkanediols according to the VPO methodology.

catalysts prepared *via* intercalation with 1,5-pentanediol and 1,6-hexanediol (VPO5, VPD5 and VPD6) gave relatively low activity (15–20%) and selectivity to maleic anhydride (22–25%). These samples were found to largely consist of V^V phases, however, bands associated with $(VO)_2P_2O_7$ were present in the Raman spectra (Fig. 9) indicating that there is disordered V^{IV} in the catalysts. These materials also have lower surface areas than the materials prepared with 1,4-butanediol.

Abon et al. [25] have shown that during catalyst activation the surface transformation of $VOHPO_4{\cdot}0.5H_2O$ to crystalline $(VO)_2P_2O_7$ occurs slowly and can initially undergo oxy-dehydration to α_{II}- and δ-$VOPO_4$, whereas the bulk of $VOHPO_4{\cdot}0.5H_2O$ undergoes a topotactic transformation to $(VO)_2P_2O_7$. In this study we found that the intercalation of α,ω-alkanediols into the precursor promotes the formation of V^V in the catalyst. This could be due to the facile delamination of the $VOHPO_4{\cdot}HO(CH_2)_nOH$ precursors leading to thin plates which are easier to oxidize under reaction conditions. This leads to a high proportion of $VOPO_4$ which is responsible for the

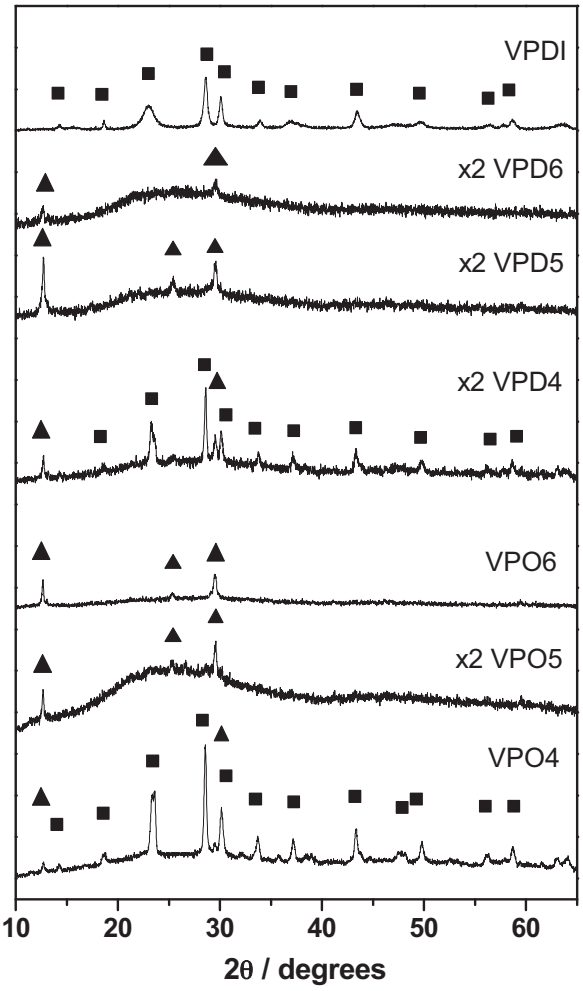

Fig. 9. XRD patterns of the vanadium phosphate materials after butane oxidation. Key: ■ $(VO)_2P_2O_7$; ▲ $VOPO_4{\cdot}nH_2O$.

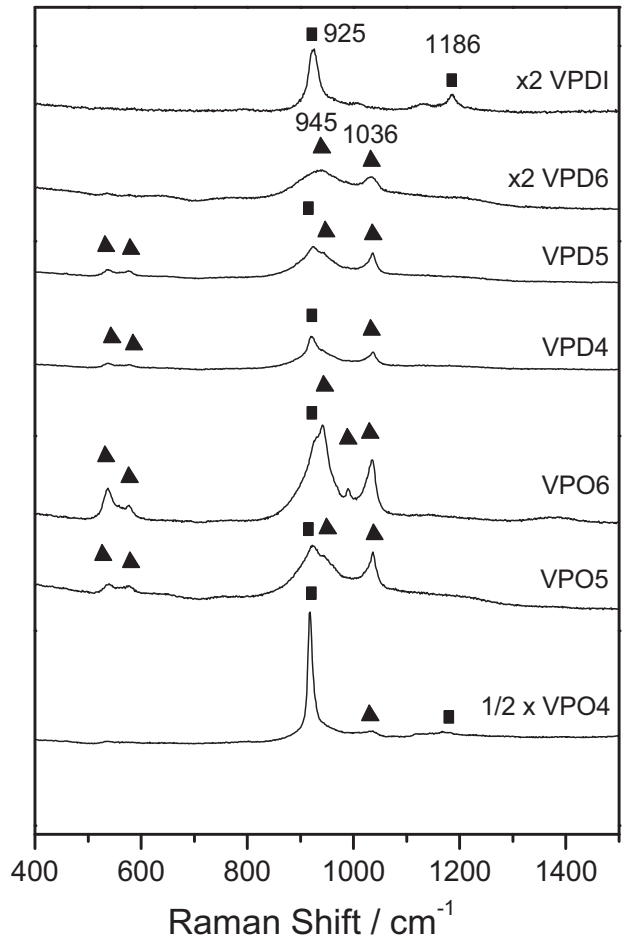

Fig. 10. Raman spectra of the vanadium phosphate materials after butane oxidation. Key: ■ $(VO)_2P_2O_7$; ▲ $VOPO_4$.

Table 2
Butane oxidation over the final catalysts.[a]

Catalyst	Butane conversion (%)	Selectivity (%)			Surface area ($m^2\ g^{-1}$)		Activity	
		MA[b]	CO	CO_2	Precursor	Final catalyst	Specific ($\times10^{-4}$) ($mol_{MA}\ g^{-1}\ h^{-1}$)	Intrinsic ($\times10^{-5}$) ($mol_{MA}\ m^{-2}\ h^{-1}$)
VPDI	50	58	23	19	23	25	2.68	1.07
VPD4	44	36	42	22	38	31	1.46	0.47
VPD5	20	24	44	32	12	12	0.44	0.37
VPD6	15	22	48	30	25	18	0.30	0.17
VPO4	59	47	34	19	22	22	2.56	1.16
VPO5	19	25	47	28	14	10	0.44	0.44
VPO6	12	22	61	17	7	6	0.24	0.41

[a] Reaction condition: 1.7% butane in air, GHSV: 3000 h^{-1}, 400 °C.
[b] MA = maleic anhydride.

poor performance and low surface area of the catalysts. As the chain length of the α,ω-alkanediol increases, the vanadium phosphate layers are further apart which makes the delamination more pronounced, leading to thinner plates which are more easily oxidized. The greater amounts of V^V in these materials are clearly observed in the XRD patterns (Fig. 9) and so the performance of the catalyst decreases.

4. Conclusions

A series of layered $VOHPO_4{\cdot}HO(CH_2)_nOH$ materials were prepared by the reduction of $VOPO_4{\cdot}2H_2O$ or V_2O_5 and H_3PO_4 with α,ω-alkanediols. The layered structure was confirmed by XRD which indicated that increasing the carbon number of the α,ω-alkanediol linearly increased the size of $d_{(001)}$. The catalysts derived from the layered $VOHPO_4{\cdot}HO(CH_2)_nOH$ showed relatively low selectivities to maleic anhydride and were found to possess large amount of V^V. This was attributed to the intercalated materials delaminating more easily to give thinner platelets which are more easily oxidized to $VOPO_4$ during the catalyst activation. $VOPO_4$ is known to be unselective for maleic anhydride production [9,25], therefore, the presence of this low surface area material decreases both the activity and the selectivity of the catalyst.

This effect was related to the chain length of the α,ω-alkanediols and in the case of 1,4-butanediol the resulting materials prepared *via* both VPO and VPD methods contained less V^V and hence performed in a comparable manner to catalysts derived from $VOHPO_4{\cdot}0.5H_2O$ precursors obtained *via* the reduction of $VOPO_4{\cdot}2H_2O$ in isobutanol.

Acknowledgements

We thank EPSRC for financial support. Xiao-Bing Fan thanks the financial support from Chinese Council of Scholarship, Cardiff University and Prof. Yuan Kou.

References

[1] R.L. Bergman, N.W. Frisch, US Patent 3,293,268 (1966).
[2] G.J. Hutchings, J. Mater. Chem. 14 (2004) 3385–3395.
[3] J.W. Johnson, D.C. Johnston, A.J. Jacobson, J.F. Brody, J. Am. Chem. Soc. 106 (1984) 8123–8128.
[4] G.J. Hutchings, A.D. Chomel, R. Olier, J.C. Volta, Nature 368 (1994) 41–45.
[5] C.J. Kiely, A. Burrows, S. Sajip, G.J. Hutchings, M.T. Sananes, A. Tuel, J.C. Volta, J. Catal. 162 (1996) 31–47.
[6] M. Ruitenbeek, A.J. van Dillen, A. Barbon, E.E. van Faassen, D.C. Koningsberger, J.W. Geus, Catal. Lett. 55 (1998) 133–139.
[7] P. Delichere, K.E. Bere, M. Abon, Appl. Catal., A 172 (1998) 295–309.
[8] F. Meunier, P. Delporte, B. Heinrich, C. Bouchy, C. Crouzet, C. Pham Huu, P. Panissod, J.J. Lerou, P.L. Mills, M.J.J. Ledoux, J. Catal. 169 (1997) 33–44.
[9] V.V. Guliants, J.B. Benziger, S. Sundaresan, I.E. Wachs, J.M. Jehng, J.E. Roberts, Catal. Today 28 (1996) 275–295.
[10] G. Centi, F. Trifiro, J.R. Ebner, V.M. Franchetti, Chem. Rev. 88 (1988) 55–80.
[11] L. O'Mahony, T. Curtin, D. Zemlyanov, M. Mihov, B.K. Hodnett, J. Catal. 227 (2004) 270–281.
[12] U. Sithamparappillai, J.L. Nuno, N.F. Dummer, W. Weng, C.J. Kiely, J.K. Bartley, G.J. Hutchings, J. Mater. Chem. 20 (2010) 5310–5318.
[13] N. Yamamoto, N. Hiyoshi, T. Okuhara, Chem. Mater. 14 (2002) 3882–3888.
[14] V.V. Guliants, J.B. Benziger, S. Sundaresan, Chem. Mater. 6 (1994) 353–356.
[15] L. Beneš, K. Melánová, V. Zima, J. Kalousová, J. Votinský, Inorg. Chem. 36 (1997) 2850–2854.
[16] S. Albonetti, F. Cavani, S. Ligi, F. Pierelli, F. Trifiró, F. Guelfi, G. Mazzoni, Stud. Surf. Sci. Catal. 143 (2002) 963–973.
[17] S. Ligi, F. Cavani, S. Albonetti, G. Mazzoni, US Patent 6,734,135 (2004).
[18] A.A. Rownaghi, Y.H. Taufiq-Yap, T.W. Jiunn, Catal. Lett. 130 (2009) 593–603.
[19] A.A. Rownaghi, Y.H. Taufiq-Yap, F. Rezaei, Ind. Eng. Chem. Res. 48 (2009) 7517–7528.
[20] M.T. Sananes, I.J. Ellison, S. Sajip, A. Burrows, C.J. Kiely, J.C. Volta, G.J. Hutchings, J. Chem. Soc. Faraday Trans. 92 (1996) 137–142.
[21] G.J. Hutchings, M.T. Sananes, S. Sajip, C.J. Kiely, A. Burrows, I.J. Ellison, J.C. Volta, Catal. Today 33 (1997) 161–171.
[22] A. Satsuma, H. Kanbe, K. Srinivasan, S. Komai, Y. Kamiya, T. Hattori, Micropor. Mesopor. Mater. 110 (2008) 528–533.
[23] Z. Xue, G.L. Schrader, J. Phys. Chem. B 103 (1999) 9459–9467.
[24] M. Trchová, P. Čapková, K. Melánová, L. Beneš, P. Matějka, E. Uhlířová, J. Solid State Chem. 148 (1999) 197–204.
[25] M. Abon, K.E. Bere, A. Tuel, P. Delichere, J. Catal. 156 (1995) 28–36.